Demo-Genetic Approach for the Conservation and Restoration of a Habitat-Forming Octocoral: The Case of Red Coral, *Corallium rubrum*, in the Réserve Naturelle de Scandola

Carlota R. Gazulla[1,2], Paula López-Sendino[1], Agostinho Antunes[3,4], Didier Aurelle[5,6], Ignasi Montero-Serra[7], Jean-Marie Dominici[8], Cristina Linares[7], Joaquim Garrabou[1,5]* and Jean-Baptiste Ledoux[1,3]*

[1] Institut de Ciències del Mar, Consejo Superior de Investigaciones Científicas, Barcelona, Spain, [2] Departament de Genètica i Microbiologia, Universitat Autònoma de Barcelona, Barcelona, Spain, [3] CIIMAR/CIMAR, Centro Interdisciplinar de Investigação Marinha e Ambiental, Universidade do Porto, Porto, Portugal, [4] Department of Biology, Faculty of Sciences, University of Porto, Porto, Portugal, [5] Aix Marseille Univ, Université de Toulon, CNRS, IRD, MIO, Marseille, France, [6] CNRS, EPHE, Institut de Systématique, Evolution, Biodiversité, Muséum National d'Histoire Naturelle, Sorbonne Université, Paris, France, [7] Departament de Biologia Evolutiva, Ecologia i Ciències Ambientals, Institut de Recerca de la Biodiversitat, Universitat de Barcelona, Barcelona, Spain, [8] Réserve Naturelle de Scandola, Parc Régional de Corse, Galeria, France

Marine protected areas (MPAs) are one of the most efficient conservation tools to buffer marine biodiversity loss induced by human activities. Beside effective enforcement, an accurate understanding of the eco-evolutionary processes underlying the patterns of biodiversity is needed to reap the benefits of management policies. In this context, integrating population genetics with demographic data, the demo-genetic approach, is particularly relevant to shift from a "species-based pattern" toward an "eco-evolutionary-based processes" conservation. Here, targeting a key species in the Mediterranean coralligenous, the red coral, *Corallium rubrum*, in an emblematic Mediterranean MPA, the "Réserve Naturelle de Scandola" (France), we applied demo-genetic approaches at two contrasted spatial scales, among populations and within one population, to (i) infer the demographic connectivity among populations in the metapopulation network and (ii) shed new light on the genetic connectivity and on the demographic transitions underlying the dynamics of a near-pristine population. Integrating different spatial and temporal scales, we demonstrated (i) an apparent temporal stability in the pattern of genetic diversity and structure in the MPA in spite of a dramatic demographic decline and (ii) contrasted levels of genetic isolation but substantial demographic connectivity among populations. Focusing on the near-pristine population, we complemented the characterization of red coral demographic connectivity suggesting (iii) temporal variability and (iv) the occurrence of collective dispersal. In addition, we demonstrated (v) contrasted patterns of spatial genetic structure (SGS), depending on the considered

stage-class (adults vs. juveniles), in the near-pristine population. This last result points out that the overall SGS resulted from a restricted dispersal of locally produced juveniles (SGS among adults and juveniles) combined to mortality during early life stages (decrease of SGS from juveniles to adults). Demonstrating the occurrence of two management units and the importance of two populations (CAVB and ALE) for the network of connectivity, we made recommendations for the management of the Réserve Naturelle de Scandola. Besides, we contributed to the implementation of scientifically driven restoration protocols in red coral by providing estimates for the size, density, and distances among patches of transplanted colonies.

INTRODUCTION

Global change is drastically modifying the networks of interactions among the different levels of marine biodiversity, from genes to ecosystems, impacting ecosystem functioning and related socioeconomic services. Marine protected areas (MPAs) are one of the most efficient tools to buffer this anthropogenic biodiversity loss. Besides an effective enforcement (Edgar et al., 2014; Costello and Ballantine, 2015), the benefits of MPAs rely on an accurate understanding of the eco-evolutionary processes shaping and maintaining the patterns of biodiversity (Sale et al., 2005). Connectivity, defined as the exchange of individuals among populations (demographic connectivity) and their successful reproduction (genetic connectivity) (Lowe and Allendorf, 2010), is of critical importance in the functioning of MPAs. It underlies the dynamics and genetics of populations (Palumbi, 2004; Gagnaire et al., 2015). However, to date, design and management of MPAs usually rely on "species-based pattern" rather than "eco-evolutionary-based processes" considerations, restraining potentially their benefits.

One way to achieve the required shift, from a pattern- to a process-focused management, relies on the integration of population genetics into conservation strategies. While this is acknowledged since the beginning of conservation biology (Soulé, 1985), population genetics and genetic diversity remain overlooked by biodiversity managers (Cook and Sgrò, 2018; Laikre et al., 2020). This is particularly detrimental considering the recent developments in demo-genetic approaches that, combining demographic information with population genetics, allow the inference of eco-evolutionary processes acting over contemporary timescale. At large spatial scale (i.e., among populations), demo-genetic approaches allow, for instance, for the estimation of contemporary connectivity (see Waples and Gaggiotti, 2006; Broquet and Petit, 2009). Populations can thus be classified in terms of their role in the functioning of the network (e.g., source vs. sink) helping, accordingly, to prioritize conservation efforts. Beside their inputs in conservation, demo-genetic approaches can be used to improve restoration practices, especially when applied at fine spatial scale (i.e., among individuals within population). In marine sessile invertebrates, the combination between the dispersive larval phase and complex reproductive strategies (Bierne et al., 2016)

can limit our understanding of ecological processes driving the population dynamics. Characterizing the fine-scale SGS within population, the non-random spatial distribution of genotypes through the formation of local pedigree structure (Vekemans and Hardy, 2004) allows to infer demographic parameters such as the "neighborhood size" (Nb) and the "mean parent-offspring distance" (σ_g) (see Rousset, 1997, Rousset, 2000). These two parameters provide insight into the distance range at which genetic interactions occurred among individuals within population (Vekemans and Hardy, 2004). Interestingly, SGS is a dynamic pattern, which can increase (e.g., Pardini and Hamrick, 2008) or decrease (e.g., Hampe et al., 2010) from juveniles to adults. Demographic processes such as density-dependent or -independent mortality during early-life stages may decrease the strength of SGS from propagule to recruit to adult-stage classes (e.g., Chung et al., 2003, 2007). Accordingly, the decomposition of SGS among stage classes can shed new light on the population dynamics of the targeted species by characterizing the interactions between the demographic and evolutionary processes shaping the pool of reproductive adults (Kalisz et al., 2001; Jacquemyn et al., 2006; Hampe et al., 2010). The characterization of the dynamics of the SGS within population and the estimation of related demographic parameters (Nb and σ_g) are thus of primary importance to support the definition of scientifically driven transplantation protocols (e.g., size and density of restored patches) and to set the size of restoration actions (e.g., distance among restored patches).

The Mediterranean Sea is a striking example of the challenges induced by global change on marine biodiversity. This biodiversity hotspot is submitted to direct anthropogenic pressures from overfishing to pollution and was recently recognized as a hotspot of climate change (Diffenbaugh et al., 2007; Cramer et al., 2018). In the last decades, mass mortality events (MMEs) linked to marine heat waves have been observed along thousands of kilometers of coastal habitats, impacting more than 90 species (Garrabou et al., 2019). Coralligenous biogenic reefs, which are among the richest Mediterranean communities (Ballesteros, 2006) and were recognized as priority habitats by the UNEP-MAP, have been particularly sensitive to MMEs (Garrabou et al., 2009, 2019). Populations of long-lived and habitat-forming macrobenthic species such as sponges, octocorals, or bryozoans were dramatically impacted by MMEs, with up to 80% of

impacted individuals in some locations (Cerrano et al., 2000; Garrabou et al., 2001, 2009, 2019). The reported high incidence and mortality rates in these key species may induce cascading effects at the ecosystem level, questioning the future of coralligenous communities (Gómez-Gras et al., 2021).

Here, focusing on red coral, *Corallium rubrum*, a key species of the Mediterranean coralligenous, in an emblematic Mediterranean MPA, the "Réserve Naturelle de Scandola" (Parc Naturel Regional de Corse, France), our main objective is to provide insight into red coral connectivity among and within populations in order to refine the management of the MPA and to contribute to the definition of scientifically driven restoration protocols. The relevance of this case study relies on two main issues. First, the Scandola Marine Reserve is one of the most emblematic MPAs in the Mediterranean. Characterized by a well-conserved biodiversity, including coralligenous habitats, and a unique and near-pristine population of red coral (Cave-b; Garrabou et al., 2017), the MPA is a reference for managers and scientists. However, little is known regarding the eco-evolutionary processes underlying the functioning of the MPA, and particularly the pattern of connectivity among populations. Then, following almost three decades of multidisciplinary studies (Abbiati et al., 1993; Santangelo et al., 1993), red coral has been established as a model species in conservation biology. This habitat-forming octocoral, with low population dynamics and late sexual maturity (Garrabou and Harmelin, 2002; Marschal et al., 2004; Torrents et al., 2005), is found in contrasted habitats mainly in the Western Mediterranean and neighboring Atlantic (Zibrowius et al., 1984; Boavida et al., 2016), from 5- to more than 1000-m depth (Knittweis et al., 2016). Warming-induced mortalities (Garrabou et al., 2001) and overharvesting for its use in jewelry (Bruckner, 2009) induced a dramatic shift in the demographic structure of shallow populations, questioning the evolutionary trajectory of the species (Montero-Serra et al., 2019). Patterns of genetic structure and diversity in shallow red coral populations have been characterized from global, to regional (including the Scandola Marine Reserve; see below), to local scales. Overall, the species shows a significant genetic structure among populations at a scale of tens of meters (Costantini et al., 2007a), which increases with geographic distance (i.e., isolation by distance pattern, IBD; Ledoux et al., 2010a; Aurelle et al., 2011; Aurelle and Ledoux, 2013). While the IBD suggests a limited gene flow occurring mainly among close-by populations, it is noteworthy that the connectivity of the species remains poorly characterized. At regional scale, some heterogeneity in the patterns of structure has been revealed (Ledoux et al., 2010a). Analyzing populations from the Scandola Marine Reserve, Ledoux et al. (2010a) revealed a lack of IBD combined to a relatively low level of genetic diversity compared to other regions. At local scale, the significant SGSs reported among individuals within an unprotected population (Ledoux et al., 2010b) suggest that red coral populations may be considered as complex networks of genetically related individuals interacting locally (few centimeters). While these data improved our abilities to restore declining populations, the eco-evolutionary processes, such as genetic connectivity and density-dependent or -independent mortality underlying the establishment of the reproductive pool

in red coral populations (Montero-Serra et al., 2015, 2018), remain to be characterized in order to provide scientifically driven restoration protocols.

Based on a sampling at the population and individual levels, we applied complementary demo-genetic approaches at two contrasting spatial scales: among populations and among individuals within one population. In a first step, we characterized the patterns of genetic diversity and structure among six red coral populations (i) to infer the demographic connectivity among these populations. In a second step, we used a geo-referenced sampling considering two stage-classes, adults vs. juveniles, (ii) to decompose the SGS in the Cave-b population, and (iii) to further characterize the potential impact of genetic connectivity and early life-stage mortality on the population dynamics of this near-pristine population. Our results suggested the occurrence of collective dispersal, improving our current knowledge regarding the ecology of *C. rubrum*. Besides, we used the genetic structure and demographic connectivity patterns to prioritize management efforts in the Scandola Marine Reserve. We translated the SGS results into restoration advices. In particular, we provided estimates for the size, density, and distance among patches to restore red coral populations.

MATERIALS AND METHODS

Sampling and Spatial Data

Established in 1975 and listed as a world heritage site in 1983 by UNESCO, the Scandola Marine Reserve (Parc Naturel Regional de Corse, France) is particularly well enforced, belonging to the 0.23% of effectively protected Mediterranean surface (Claudet et al., 2020). In this MPA, individuals of *C. rubrum* from six populations were collected by SCUBA diving at depths from 15 to 25 m between 2015 and 2017 (**Figure 1A**). In five populations separated by distance ranging from 20 m to less than 2 km (DHM, ALI, ALE, PPL, and PLU), apical fragments (~5 mm) from 30 to 51 mature individuals (i.e., colonies higher than 30 mm; Torrents et al., 2005) were randomly sampled. In Cave-b (CAVB), sampling was conducted following a 6.25-m-length horizontal transect at a depth of 23 m. Based on its demographic structure showing the highest biomass reported to date in the Mediterranean Sea (more than 100-fold) and the coexistence of a high number of juveniles, low size, and large centennial colonies in high density (201 colonies*m^{-2}), the Cave-b population is a unique and near-pristine population of red coral (Garrabou et al., 2017). The high density of this population combined to the morphological characteristics of the habitat prevents a georeferenced sampling at the individual level. Accordingly, 11 quadrats (25 × 25 cm) were sampled. The size of the quadrat was of the same order as the mean square parent–offspring distance (σ_g) estimated by Ledoux et al. (2010b). Nine quadrats were sampled every 50 cm along the transect. Two quadrats at the center of the transect were duplicated 25 cm above the transect. Within each quadrat, 15–20 adult colonies and a similar number of juvenile colonies were randomly collected (see **Figure 1B** and **Table 1**). In the red coral, sexual maturity was reported in colonies higher than 30 mm (Torrents et al., 2005). To

avoid potential mis-assignment in the reproductive status of the samples, we considered adult and juvenile colonies as colonies higher than 100 mm and between 5 and 10 mm, respectively. For the adult colonies, small fragments (<10 mm) were sampled while, for the juveniles, the whole colonies were sampled.

The resulting 634 apical fragments were conserved in 95% ethanol and stored at −20°C prior to DNA extraction.

DNA Extraction, Microsatellite Genotyping, and Quality Control

DNA extraction, microsatellite genotyping, and quality control are described in **Supplementary Material**. Briefly, all the individuals were genotyped using eight microsatellite loci amplified in three multiplexes: Multiplex 1 (Mic13/Mic20/Mic26), Multiplex 2 (Mic24/Mic25/Mic27), and Multiplex 3 (Mic22/Mic23) (Ledoux et al., 2010a). Following the quality control, statistical analyses were conducted with a dataset including 580 colonies, corresponding to the same number of unique multilocus genotypes, including 201 adults (CAVB-AD) and 166 juveniles (CAVB-JUV) from Cave-b and 213 individuals from five populations (**Table 1**).

Hardy–Weinberg Equilibrium and Genetic Diversity

Probability of identity (Pi; the average probability that two samples will share the same genotype), Hardy–Weinberg equilibrium, and genetic diversity analyses for each population, including total number of alleles, observed (H_o) and unbiased heterozygosity (H_e; Nei, 1973), f estimator of F_{IS}, and rarefied allelic richness ($Ar_{(56)}$; Petit et al., 1998), are described in **Supplementary Material**.

SGS Among Populations

A clustering analysis using STRUCTURE 2.2 (Pritchard et al., 2000) was conducted to evaluate the number of genetic clusters (K) from the individuals' genotypes without assumptions on population boundaries and considering the whole dataset. Because of the unbalanced sampling, we considered the admixture model with correlated allele frequencies (Falush et al., 2003, 2007) and population-specific ancestry prior (α) with an $\alpha = 0.17$ (=1/number of assumed populations; Wang, 2017). Ten independent runs were performed for each K with a burn-in period of 500,000 followed by 250,000 iterations. The K-value corresponding to "upper most hierarchical level of structure" was determined using Ln Pr(X| K) (Pritchard et al., 2000), the ΔK method (Evanno et al., 2005), and the MedMedK, MedMeaK, MaxMedK, and MaxMeaK statistics with three different thresholds (0.6, 0.7, and 0.8; Puechmaille, 2016), CLUMPP 1.1 (Jakobsson and Rosenberg, 2007), and DISTRUCT 1.1 (Rosenberg, 2003) were used for graphical outputs.

We conducted a discriminant analysis of principal components (DAPC, Jombart et al., 2010) in ADEGENET (Jombart, 2008). Contrary to STRUCTURE, DAPC describes patterns of diversity without assumption about the underlying population genetic model (Jombart et al., 2010). Data were transformed into principal components, and discriminant analyses were used to maximize variation among groups while minimizing variations within the group. We used the seven population locations (discriminating here among adults and juveniles from CAVB) as group prior. Based on the *a-score* method, the number of principal components was set to 46, while we retained three discriminant functions.

Global and pairwise differentiations were quantified using Weir and Cockerham's (1984) estimators of F_{ST} in GENEPOP (Rousset, 2008). Genotypic differentiation was tested using an exact test based on the MC algorithm (Guo and Thompson, 1992) with default parameters in GENEPOP.

Isolation by distance among populations was tested using a linear regression of genetic distances computed as $F_{ST}/(1 - F_{ST})$ over logarithms of the geographic distances ($ln(d)$) (Rousset, 1997). The significance of the correlation between the genetic distances ($F_{ST}/(1 - F_{ST})$) and the logarithms of geographic distances (Ln(d)) was tested by the Mantel test with 10,000 permutations in GENEPOP.

We used GESTE (Foll and Gaggiotti, 2006) to compute the population-specific F_{ST}. Measuring the genetic differentiation of each population, this method gives insight into the relative impact of genetic drift on the differentiation of the considered population (Gaggiotti and Foll, 2010).

Assignment Tests

Two sets of assignment tests in GeneClass2 (Piry et al., 2004) were conducted in order to (i) estimate the demographic connectivity among the six populations (not considering juveniles from CAVB) and (ii) detect migrants within the juveniles sampled in CAVB. First, we conducted a filtered assignment analysis following Lukoschek et al. (2016). We identified first-generation migrants (FGMs) in each population using the Bayesian criteria of Rannala and Mountain (1997) with 100,000 simulated genotypes and an alpha of 0.005. FGMs were removed from the dataset and reassigned to the reference dataset (i.e., dataset without FGMs). Migrants were assigned to a population if their assignment probability was >0.01. We allowed for multiple assignments (i.e., one individual originating potentially from different populations). When the assignment probability of an FGM was lower than 0.01 for all populations, we considered this FGM to come from an unsampled population.

Then, focusing on CAVB, we assigned CAVB-JUV considering the remaining samples (i.e., five populations + CAVB-AD) as reference. We used the Bayesian assignment method of Rannala and Mountain (1997) simulating 100,000 individuals and an alpha of 0.005. Following this analysis, CAVB-JUV was divided in two samples, CAVB-JUV-L and CAVB-JUV-M, distinguishing the juveniles originating from CAVB (locally produced) from the immigrant juveniles, respectively.

Fine-Scale SGS and Neighborhood Size

Focusing on CAVB, we analyzed the SGS by regressing the Nason's kinship coefficients (F_{ij}; Loiselle et al., 1995) among pairs of individuals on the logarithms of pairwise geographic distances, in SPAGEDI (Hardy and Vekemans, 2002). We first conducted this analysis considering a "global dataset" including CAVB-AD and CAVB-JUV-L. Then, we decomposed the SGS
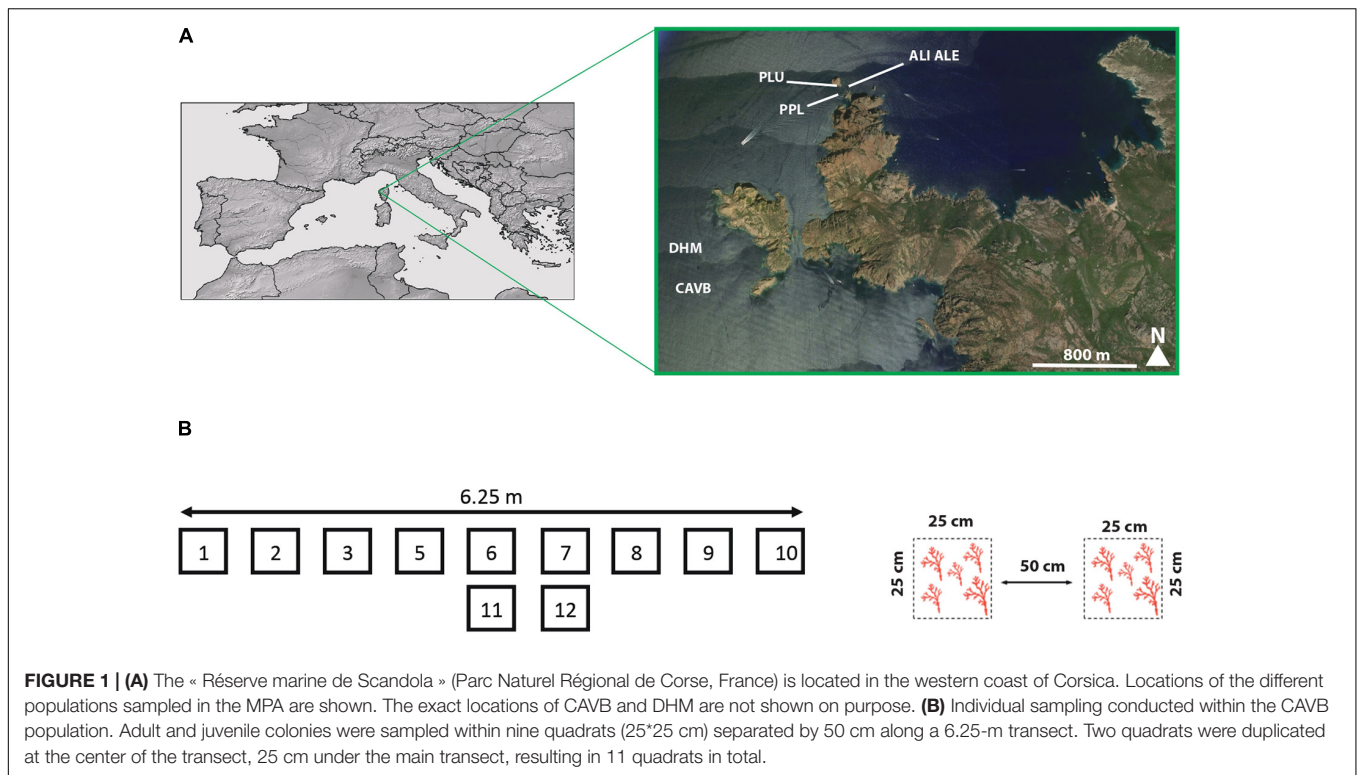
FIGURE 1 | (A) The « Réserve marine de Scandola » (Parc Naturel Régional de Corse, France) is located in the western coast of Corsica. Locations of the different populations sampled in the MPA are shown. The exact locations of CAVB and DHM are not shown on purpose. **(B)** Individual sampling conducted within the CAVB population. Adult and juvenile colonies were sampled within nine quadrats (25*25 cm) separated by 50 cm along a 6.25-m transect. Two quadrats were duplicated at the center of the transect, 25 cm under the main transect, resulting in 11 quadrats in total.

TABLE 1 | Location and genetic diversity estimators of the *Corallium rubrum* populations.

Population	Label	N	Latitude	Longitude	r	H_o	H_e	F_{IS}	$Ar_{(56)}$	Population-specific F_{ST} [95% CI]
Cave b	CAVB-AD	201	42°22′50″N	8°32′48″E	0.11	0.50	0.69	**0.25**	10.77	0.055 [0.044–0.067]
	CAVB-JUV	166					0.53	0.68	**0.22**	10.57	
Droite Harmelin	DHM	41	42°22′50″N	8°32′48″E	0.11	0.50	0.67	**0.24**	11.36	0.057 [0.041–0.075]
Corail Albinos extérieur	ALE	44	42°22′48″N	8°32′51.324″E	0.09	0.58	0.73	**0.22**	11.3	0.050 [0.036–0.067]
Corail Albinos intérieur	ALI	30	42°22′48″N	8°32′51.324″E	0.13	0.51	0.72	**0.30**	10.91	0.053 [0.035–0.072]
Grotte Palazzu	PLU	49	42°22′48.72″N	8°32′46.86″E	0.09	0.59	0.73	**0.20**	9.71	0.097 [0.070–0.123]
Passe Palazzu	PPL	49	42°22′47.64″N	8°32′51.288″E	0.09	0.57	0.72	**0.19**	9.81	0.079 [0.058–0.102]

N, number of individuals; r, frequency of null alleles estimated with FreeNa; H_o, observed heterozygosity; H_e, gene diversity (Nei, 1973); F_{IS}, following Weir and Cockerham (1984); $Ar_{(56)}$, rarefied allelic richness considering 56 genes. Population-specific F_{ST} and 95% CI. For Cave b (CAVB) and Droite Harmelin (DHM) samples, we only provided approximate coordinates. For Cave b, H_o, H_e F_{IS}, and $Ar_{(56)}$ are given for adults and juveniles. Bold values for F_{IS} correspond to populations where significant heterozygote deficiencies were observed (p-Values < 0.001). No significant difference was observed among adults and juveniles when comparing H_o, H_e F_{IS}, and $Ar_{(56)}$ (all p-Values > 0.05).

by conducting the same analyses considering three categories: CAVB-AD, CAVB-JUV-L, and a "between-generation" (i.e., each pair is composed by one juvenile and one adult), referring to allele frequencies within each group. In each case, significance of the slope of the linear regression (b) was tested using 10,000 permutations. The pattern of SGS was represented with a correlogram using eight distance classes ([0–25]; [25–75]; [75–150]; [150–231]; [231–300]; [300–376]; [376–451]; [451–625]). Approximate confidence intervals (95%) for average kinship values for each spatial distance were obtained by permuting individual locations 10,000 times. Differences in SGS among the different categories were assessed using the Sp statistics with $Sp = -b/(1 - \hat{F}_{(1)})$, with $\hat{F}_{(1)}$ being the mean F_{ij} among individuals belonging to the first distance interval (Vekemans and Hardy, 2004).

For the global dataset (CAVB-AD and CAVB-JUV-L), we computed the neighborhood size (N_b) as $N_b = 1/Sp$ and we deduced the moment estimate of the mean parent–offspring distance, σ_g, from $N_b = 4*\pi*D_e*\sigma_g^2$ (see Rousset, 1997) with the effective density, $D_e = 201$ ind*m^{-2} (all adult colonies take part in reproductive events; Garrabou et al., 2017) and $D_e = 100$ ind*m^{-2} (half of the adult colonies take part in reproductive events).

Sibship and Parentage Analysis

We characterized the pattern of relationships combining three different methods and considering two sets of individuals: (i) CAVB-JUV-L and CAVB-AD and (ii) CAVB-JUV-M.

First, we used the F_{ij} Nason's kinship coefficients. Theoretically, F_{ij} discriminates among different types of relationships: $F_{ij} = 0.25$ or $F_{ij} = 0.125$ is expected for full-sibs and half-sibs, respectively. However, depending on allele frequencies, F_{ij} is influenced by the polymorphism of the molecular markers. We conducted simulations based on the allele frequencies accounting for the six populations to estimate F_{ij} values linked to four levels of relationships: unrelated (UN), half-sibs (HS), full-sibs (FS), and parent-offspring (PO). RELATED R-package (Pew et al., 2015) was used to simulate 1,000 pairs of genotypes for each of the four categories. This allowed us to define threshold values for the different categories of relationships (see section "Results"). We then computed pairwise F_{ij}s within CAVB-JUV-L, within CAVB-JUV-M, and between CAVB-JUV-L and CAVB-AD, referring to the allele frequencies of the whole dataset, and we used the threshold values to characterize the pattern of relationships.

The maximum-likelihood method implemented in COLONY 2.0.6.1 (Jones and Wang, 2010) was used to reconstruct the parental relationships among individuals based on their multilocus genotypes. COLONY reconstructs sibship and assigns paternity jointly considering the likelihood over the entire pedigree. Analyses were conducted considering two sets of individuals (i.e., CAVB-JUV-L/CAVB-AD and CAVB-JUV-M). For each set, we conducted three runs with different seed numbers considering females and males as polygamous and using the full-likelihood method with very high likelihood precision and very long length of run. For the first set, individuals from CAVB-AD were considered as potential fathers or mothers, while the second set was conducted without potential parents.

The two methods showed contrasted results with a low number of concordant relationships, which may be explained by different factors such as the presence of null alleles. Accordingly, we contrasted the results obtained with the two methods in a third step, using the statistical approach implemented in ML-Relate (Kalinowski et al., 2006). The analysis based on F_{ij} involving a high number of pairs (>60,000), we thus focused on juveniles and, more particularly, on juveniles with $F_{ij} > 0.2625$ and on adult/juvenile pairs with $F_{ij} > 0.4228$ (see section "Results"). Regarding COLONY, we accounted for all the inferred HS, FS, and PO relationships. Overall, the first two methods identified 28 PO, 193 HS, and 16 FS relationships (see section "Results"). For each of the relationships identified with one method but not with the other, we considered the identified relationship as the putative relationship and the UN relationship as the alternative relationship in ML-Relate. The putative relationship was tested based on the sampling distribution of a test statistic obtained after simulations of 1,000 genotypes under the alternative hypothesis (see Kalinowski et al., 2006 for details).

RESULTS

Hardy–Weinberg Equilibrium and Genetic Diversity Estimators

Significant linkage disequilibrium after FDR correction was observed between *Mic13* and *Mic25* when considering all populations. However, no significant disequilibrium was observed when considering each population separately. The estimated frequency of null alleles was between 0.09 for PPL and 0.13 for ALI (mean over populations $\pm$ SE = 0.10 $\pm$ 0.01). The probability of identity (*Pi*) was $2.6 * 10^{-11}$, supporting the validity of the set of microsatellites to infer relationships among individuals. Observed heterozygosity values were between 0.50 for DHM and 0.59 for PLU (mean over populations $\pm$ SE = 0.54 $\pm$ 0.04). The gene diversity H_e ranged between 0.67 (DHM) and 0.74 (ALE) (mean over populations $\pm$ SE = 0.71 $\pm$ 0.02). The f estimator of F_{IS} varied between 0.19 (PPL) and 0.23 (CAVB-AD) (mean over populations $\pm$ SE = 0.23 $\pm$ 0.04). Significant departure from panmixia was observed in all populations (significant *p*-Value after FDR correction). The lowest and highest values of $Ar_{(56)}$ were observed for PLU (9.71) and DHM (11.36) (mean $Ar_{(56)}$ over populations $\pm$ SE = 10.63 $\pm$ 0.65) (see **Table 1**). None of the genetic diversity estimators was significantly different among CAVB-AD vs. CAVB-JUV (all *p*-Values > 0.05).
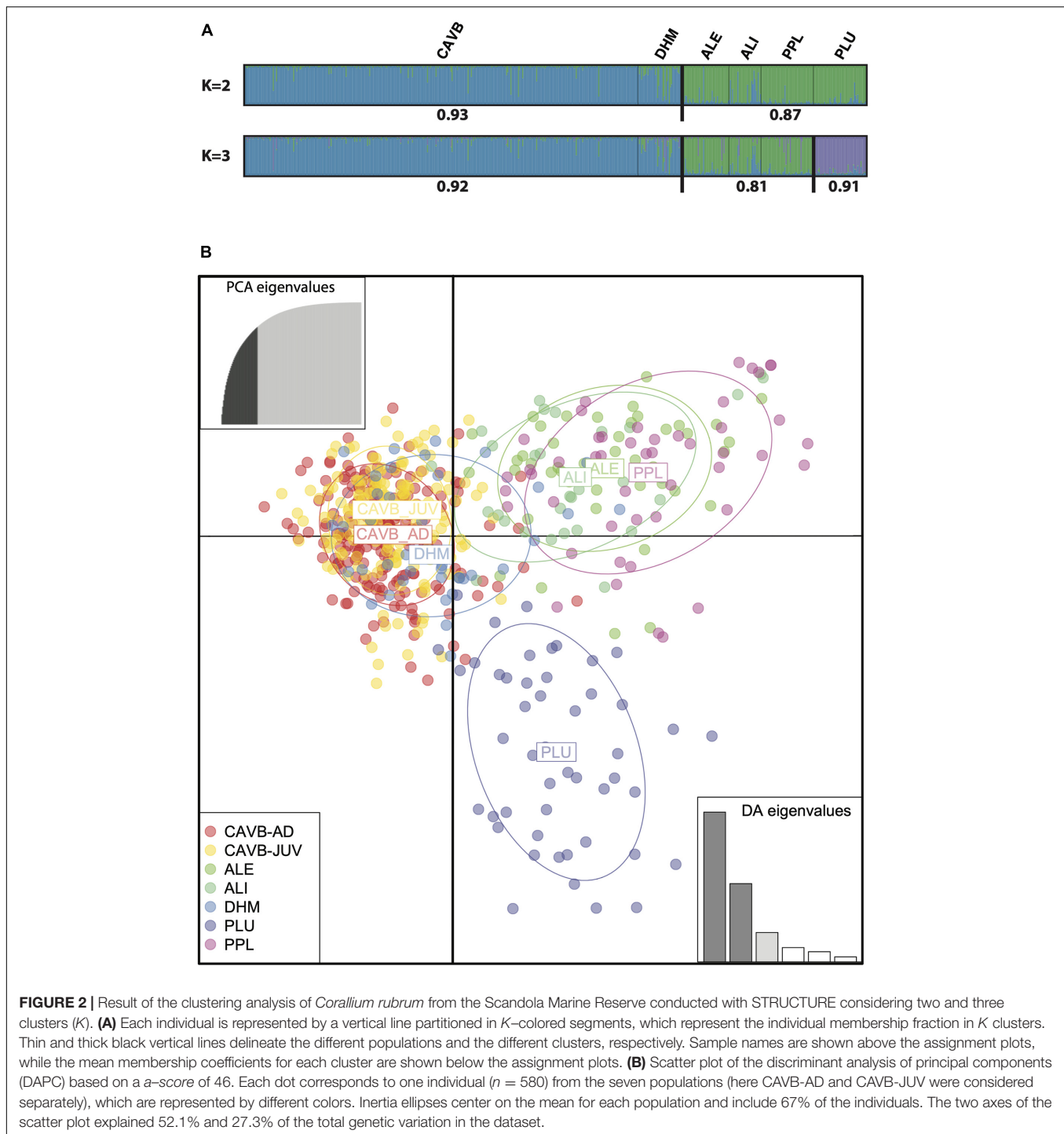
SGS Among Populations

L*nP(D)* increased slightly for the whole range of considered *K*-values (i.e., no plateau) with the strongest increases observed for $K = 2$ and $K = 3$. Evanno's method (Evanno et al., 2005) identified two different genetic clusters, while Peuchmaille statistics supported $K = 2$ (median/mean with threshold 0.7 and 0.8) and $K = 3$ (remaining statistics) (**Figure 2A**; **Supplementary Material**). For $K = 2$, the first cluster encompassed all the individuals from CAVB and DHM (mean membership coefficient = 0.93). The remaining individuals were grouped in a second cluster with a relatively high mean membership coefficient (0.87). When considering $K = 3$, this second cluster was divided in two clusters segregating the individuals from PLU (mean membership coefficient = 0.91). Those results were consistent considering null alleles as recessive alleles or missing data (data not shown).

In the DAPC analyses, individuals from CAVB and DHM were separated from the remaining individuals along the first axis, while the second axis separated the individuals from PLU from the individuals from ALI, ALE, and PPL. Those two axes represented 79.4% of the total variation in the data (**Figure 2B**).

The global F_{ST} was 0.069. The pairwise F_{ST}s ranged from 0.022 for ALI vs. ALE to 0.124 for CAVB vs. PLU. The genetic distance ($F_{ST}/(1 - F_{ST})$) and the geographic distance ($Ln(d)$) were not correlated rejecting the IBD among the six populations (*p*-Value = 0.22). The exact tests for genotypic differentiation were significant at the global level and for all pairwise comparisons except between ALI and ALE, separated by 20 m (see **Supplementary Material**). Regarding the temporal differentiation, the pairwise F_{ST} between CAVB-AD and CAVB-JUV was low (0.001), but the genotypic differentiation was significant (*p*-Value < 0.01).

The lowest population-specific F_{ST} was observed for ALE (0.050; 95% CI: 0.036–0.067) whereas the highest value was observed for PLU (0.097; 95% CI: 0.070–0.123). Based on 95%
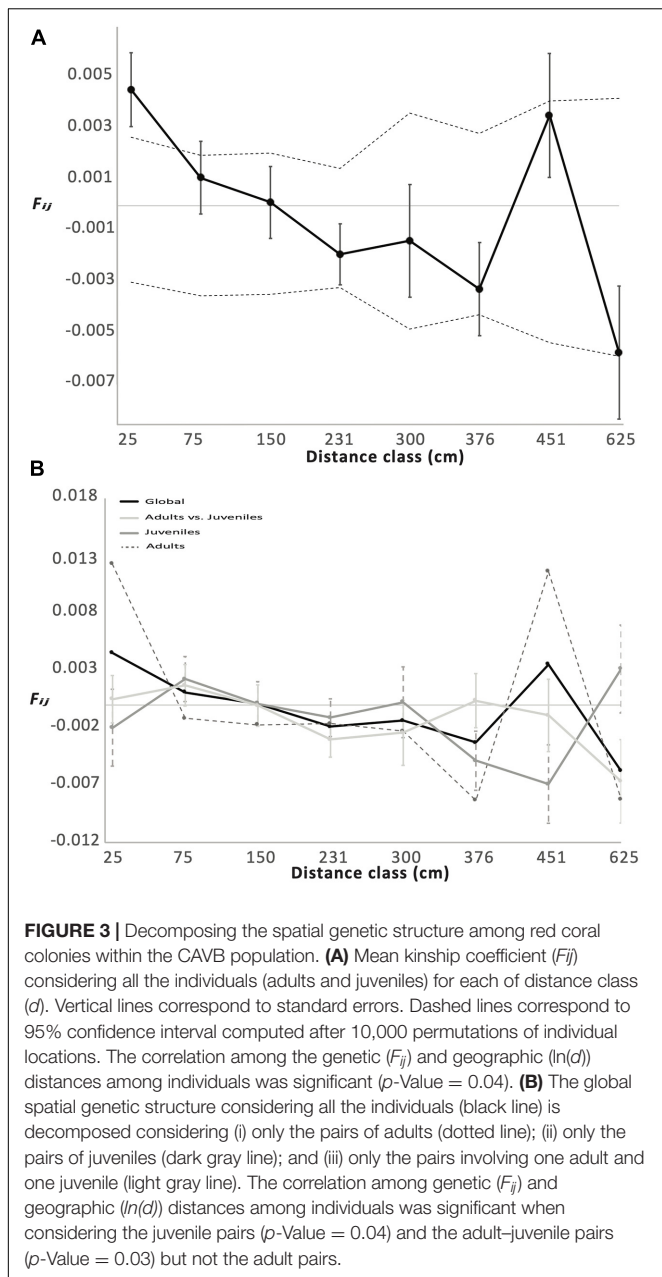
FIGURE 2 | Result of the clustering analysis of *Corallium rubrum* from the Scandola Marine Reserve conducted with STRUCTURE considering two and three clusters (*K*). **(A)** Each individual is represented by a vertical line partitioned in *K*–colored segments, which represent the individual membership fraction in *K* clusters. Thin and thick black vertical lines delineate the different populations and the different clusters, respectively. Sample names are shown above the assignment plots, while the mean membership coefficients for each cluster are shown below the assignment plots. **(B)** Scatter plot of the discriminant analysis of principal components (DAPC) based on a *a–score* of 46. Each dot corresponds to one individual (*n* = 580) from the seven populations (here CAVB-AD and CAVB-JUV were considered separately), which are represented by different colors. Inertia ellipses center on the mean for each population and include 67% of the individuals. The two axes of the scatter plot explained 52.1% and 27.3% of the total genetic variation in the dataset.

CI, significantly different population-specific F_{ST}s were observed for PLU vs. CAVB and PLU vs. ALE (**Table 1**).

Assignment Tests

Considering the whole dataset, 69 of the 419 individuals (16.4%) were identified as FGM, with eight (PPL) to 15 (DHM) FGMs per population. Considering assignment probability > 0.01 and allowing for multiple assignments, we assigned seven FGMs

(10.1%) to three populations (CAVB, ALE, and PPL) indicating that 89.9% of the FGMs came from unsampled populations. Three populations (DHM, ALI, and PLU) did not produce any FGM. From the assigned FGMs, 50% came from CAVB.

When focusing on CAVB, 17 juveniles were not assigned to CAVB-AD (i.e., assignment probability < 0.005), while 10 juveniles were assigned to one of five other populations, with a probability higher than the assignment probability to CAVB-AD.

FIGURE 3 | Decomposing the spatial genetic structure among red coral colonies within the CAVB population. **(A)** Mean kinship coefficient (F_{ij}) considering all the individuals (adults and juveniles) for each of distance class (d). Vertical lines correspond to standard errors. Dashed lines correspond to 95% confidence interval computed after 10,000 permutations of individual locations. The correlation among the genetic (F_{ij}) and geographic (ln(d)) distances among individuals was significant (p-Value = 0.04). **(B)** The global spatial genetic structure considering all the individuals (black line) is decomposed considering (i) only the pairs of adults (dotted line); (ii) only the pairs of juveniles (dark gray line); and (iii) only the pairs involving one adult and one juvenile (light gray line). The correlation among genetic (F_{ij}) and geographic (ln(d)) distances among individuals was significant when considering the juvenile pairs (p-Value = 0.04) and the adult–juvenile pairs (p-Value = 0.03) but not the adult pairs.

Accordingly, those 27 juveniles were considered as migrants. Considering only assignment probability higher than 0.01, nine of these 27 (33.3%) migrants were assigned to DHM. The 18 remaining migrants were considered as coming from unsampled population(s) (assignment probability < 0.01 in all populations).

Fine-Scale SGS

We demonstrated an overall SGS based on the marginally significant and negative correlation between Nason's kinship coefficients (F_{ij}) and $ln(d)$ observed when considering the "global dataset" ($b = -1.7 * 10^{-3}$; p-Value = 0.04). From the neighborhood size ($Nb = 575.3$ individuals), we estimated the mean parent–offspring distance $\sigma_g = 15.09$ cm and 21.39 cm

for $D_e = 201$ individuals*m^{-2} and $D_e = 100$ individuals*m^{-2}, respectively. The decrease in kinship with geographic distance remained significant considering the CAVB-JUV-L dataset ($b = -2.4*10^{-3}$; p-Value = 0.03) and the CAVB-AD/CAVB-JUV-L dataset ($b = -2.2*10^{-3}$; p-Value = 0.04). No significant correlation was observed ($b = -8.2*10^{-4}$; p-Value = 0.29) when considering CAVB-AD. In spite of a trend toward stronger SGS for CAVB-JUV-L and CAVB-AD/CAVB-JUV-L ($Sp = 0.0024$ and 0.0022, respectively) compared to the whole dataset ($Sp = 0.0017$), no significant difference in Sp was observed (**Figure 3** and **Table 2**).

Sibship and Parentage Analysis

The pairwise F_{ij} values for simulated unrelated (UN), halfsibs (HS), fullsibs (FS), and parent–offspring (PO) ranged from −0.1984 to 0.2625 (mean ± SD = −0.001 ± 0.071), −0.1160 to 0.4228 (0.126 ± 0.087), −0.0246 to 0.6393 (0.248 ± 0.106), and 0.0622 to 0.6556 (0.252 ± 0.077), respectively. Considering the overlaps of simulated F_{ij} distributions for the four categories of relationships (see **Supplementary Material 4**), we distinguished UN ($F_{ij} < -0.1160$) from related (HS, FS, and PO) pairs ($F_{ij} > 0.2625$). Within the related pairs, juvenile pairs with $0.2625 < F_{ij} < 0.4228$ were considered as HS or FS. Finally, pairs with $F_{ij} > 0.4228$ were assigned to PO or FS depending on whether they involved one adult/one juvenile or two juveniles, respectively. Note that some pairs (e.g., all the pairs with −0.1160 < F_{ij} < 0.2625) were not further considered since we were unable to assign a relationship category.

For the 351 pairs involving the 27 migrant juveniles (CAVB-JUV-M), the mean F_{ij} (±SD) was 0.0084 (0.1124). We identified eight related pairs ($F_{ij} > 0.2625$; 2.2%), from which seven were considered as HS or FS ($0.2625 < F_{ij} < 0.4228$; 1.9%) and one as FS ($F_{ij} > 0.4228$; 0.3%). Forty pairs were considered as UN ($F_{ij} < -0.1159$; 11.4%). UN and HS pairs occurred among juveniles belonging to the same or to different quadrats, while the FS involved individuals sampled within the same quadrat.

When considering 139 local juveniles (CAVB-JUV-L), the mean F_{ij} (±SD) was 0.0166 (0.0981). Among the 9,591 pairs, 689 (7.18%) were considered as UN ($F_{ij} < -0.1159$), while 153 HS or FS ($0.2625 < F_{ij} < 0.4228$; 1.6%) and six FS ($F_{ij} > 0.4228$; 0.06%) pairs were revealed. Two FS pairs involved juveniles sampled at the two extremes of the transect while 66 UN pairs involved juveniles sampled in the same quadrat.

The mean F_{ij} (±SD) among adults (CAVB-AD) was 0.0086 (0.1007). Among the 20,100 pairs, we identified 1761 (8.76%) UN ($F_{ij} < -0.1159$) and 329 (1.63%) related ($F_{ij} > 0.2625$) pairs. From the related pairs and considering the CAVB-AD samples involving different generations, 306 (1.52%) were considered as HS or similar second-degree relatives (e.g., grand-parent/grand-offspring, avunculate) ($0.2625 < F_{ij} < 0.4228$), while 23 (0.01%) were considered as FS or first-degree relatives ($F_{ij} > 0.4228$).

The mean F_{ij} (±SD) for CAVB-AD vs. CAVB-JUV-L was 0.0104 (0.0990). Among the 30,351 pairs, we identified 2,629 (8.66%) UN ($F_{ij} < -0.1159$) and 412 (1.35%) related ($F_{ij} > 0.2625$) pairs. From the related pairs, 387 (1.52%) were considered as HS or similar degree relationships

TABLE 2 | Decomposing the spatial genetic structure among individuals within Cave-b population: Summary statistics of the regression analyses between the geographic ($ln(d)$) and genetic (F_{ij}) distances among pairs of individuals.

	Global		Adults vs. juveniles		Adults		Juveniles	
	Moment estimate	95% CI	Moment estimate	95% CI	Moment estimate	95% CI	Moment estimate	95% CI
b	**-0.0017**	−0.0020; 0.0016	**-0.0023**	−0.0025; 0.0029	−0.0009	−0.0050; 0.0033	**-0.0023**	−0.0026; 0.0023
F_1	0.0045	−0.0030; 0.0027	0.0005	−0.0050; 0.0031	0.0123	−0.0054; 0.0048	−0.0019	−0.0069; 0.0061
Sp	0.0017	−0.0016; 0.0020	0.0023	−0.0029; 0.0025	0.0009	−0.0034; 0.0049	0.0023	−0.0023; 0.0025
Nb (individuals)	575.28							
σ^2_g (cm) $D_e = 201$ individus*m^{-2}	15.09							
σ^2_g (cm) $D_e = 100$ individus*m^{-2}	21.39							

We considered alternatively (i) all the individual pairs (Global); (ii) only individual pairs involving one adult and one juvenile (Adults vs. Juveniles); (iii) only individual pairs involving two adults (Adults); and (iv) individual pairs involving two juveniles (Juveniles). b: slope of the linear regression (in bold significant value at 0.05); $F_{(1)}$ the mean F_{ij} between individuals belonging to the first distance interval; Sp statistics with $Sp = -b/(1 - \overline{F}_{(1)})$ (see Vekemans and Hardy, 2004). For the regression involving all the individuals (Global), we computed the neighborhood size (Nb) and the mean parent–offspring distance (σ^2_g) considering two different values of effective density (D_e).

$(0.2625 < F_{ij} < 0.4228)$, while 25 (0.08%) were considered as PO ($F_{ij} > 0.4228$).

Regarding COLONY analyses, no HS and two (0.6%) FS pairs ($p > 0.6$) were observed in migrant juveniles (CAVB-JUV-M). Considering local juveniles (CAVB-JUV-L) and adults (CAVB-AD), 10 (0.1%) FS and 40 (0.4%) HS pairs were identified ($p > 0.6$) in addition to three PO pairs. All the PO pairs involved the same parent.

Filtering these results using the statistical test implemented in ML-Relate, we retained 114 HS, 7 FS among the local juveniles (CAVB-JUV-L), and 11 PO pairs when considering the adults. Within the migrant juveniles (CAVB-JUV-M), two HS and one FS pairs were retained.

DISCUSSION

Genetic Diversity and Structure in the Scandola Marine Reserve: Apparent Stability of the Diversity Pattern in Spite of a Dramatic Demographic Decline

We used complementary approaches to characterize the SGS among six red coral populations in the Scandola Marine Reserve. When considering the clustering approach, the first level of structure ($K = 2$) supports the occurrence of a geographic break among the northern (PLU, PPL, ALI, and ALE) and southern (CAVB and DHM) populations with high membership coefficients (0.87 and 0.93, respectively). For $K = 3$, individuals from PLU were segregated from the individuals from PPL, ALI, and ALE forming two subclusters, also characterized by high membership coefficients (0.91 and 0.81, respectively). This pattern was fully supported by the DAPC analyses, which discriminated among northern and southern populations along the first axis (52.1%), while individuals from PLU were separated from PPL, ALI, and ALE along the second axis (27.3%). When shifting at the population level, we found significant genotypic

differentiation among all population pairs, with the exception of ALE vs. ALI, which belong to the same location (only apart by 15 m). Worthy of note is that the genetic distances between populations were not correlated with the geographic distances, rejecting the isolation-by-distance pattern (IBD). Computations of the population-specific F_{ST}s identified PLU as genetically isolated, compared to the remaining populations, which showed relatively homogenous values. Accordingly, a geographic imprint explains part of the global pattern (i.e., northern vs. southern clusters). Yet, the differentiation of PLU points out the importance of local genetic drift effects in the survey area, which may potentially explain the lack of IBD usually reported in this species (e.g., Ledoux et al., 2010a; Aurelle et al., 2011). Non-exclusive hypotheses can explain this genetic differentiation of PLU. Located in a cave, PLU can be isolated from neighboring populations due to hydrodynamic factors (e.g., Costantini et al., 2018). PLU is also impacted by a dramatic demographic decline with more than 90% of biomass lost during the last 15 years due to warming-induced MMEs (Gómez-Gras et al., 2021). This decline can potentially increase the effect of genetic drift in this particular population.

Overall, the pattern reported here, combining different genetic clusters with a lack of IBD, matches the pattern previously reported in the same region almost 10 years ago (Ledoux et al., 2010a). The same happens for the genetic diversity estimators, with values estimated here similar to previously reported values (Ledoux et al., 2010a). Changes in heterozygosity values are difficult to detect (Riquet et al., 2017), and a delay in the detection of genetic erosion is expected in long-lived species with overlapping generations such as red coral (e.g., Hailer et al., 2006). However, this apparent stability in the pattern of genetic structure and diversity remains surprising considering the dramatic demographic decline reported in red coral in this area (Gómez-Gras et al., 2021). While deserving cautious interpretation, this result highlights the need to consider complementary metrics such

as effective population sizes to characterize temporal trend in genetic diversity.

Integrating "Among Populations" and "Within Population" Demo-Genetic Approaches: Demographic Connectivity of Red Coral in the Scandola Marine Reserve

Our analyses suggested substantial demographic connectivity among the studied populations. Indeed, 16.4% of the mature individuals were identified as FGMs, in the six populations, including the drifting population of PLU. This result may appear counterintuitive in the context of the significant genetic structure observed even between populations separated by tens of meters (e.g., PPL vs. ALE). However, it is supported by recent studies in other Mediterranean octocorals reporting some levels of contemporary connectivity at least during recolonization steps (e.g., Arizmendi-Mejía et al., 2015; Padrón et al., 2018; Aurelle et al., 2020). Conciliating these, *a priori*, contradictory results imply further studies such as a detailed characterization of the balance between genetic drift and gene flow, during the course of population succession (i.e., from colonization to senescence). We hypothesize that the genetic imprint of migrants on a population will decrease from colonization to population maturation due to an increase of the genetic imprint of locally produced recruits. Our current understanding of the colonization processes (see below) combined to a potential underestimation of the influence of genetic drift on the patterns of spatial structure in *Corallium rubrum*, and other octocorals (Ledoux et al., 2015; Crisci et al., 2017; Pratlong et al., 2018) are in line with this hypothesis. Low reproductive success of migrants (i.e., limited genetic connectivity), due for instance to microenvironmental conditions favoring locally produced genotypes (e.g., Gorospe and Karl, 2013), may be another hypothesis to explore to solve this apparent paradox.

Following the filtering assignment, most of the FGMs identified (89.9%) came from unsampled populations. When considering the assigned migrants, two populations (CAVB and ALE) were identified as the main sources in the population network. In spite of a lack of isolation by distance, most of these assigned migrants came from neighboring populations separated by tens of meters (e.g., from CAVB to DHM), suggesting a low level of demographic connectivity among the Northern and Southern main genetic clusters. These analyses also support that the pool of migrants identified in each population came from (at least two) different sources. Accordingly, the multiple origins of migrants demonstrated in recently colonized and mature populations of other Mediterranean octocorals (*Paramuricea clavata and Eunicella cavolini*; see Mokhtar-Jamaï et al., 2011; Arizmendi-Mejía et al., 2015; Ledoux et al., 2018; Padrón et al., 2018; Aurelle et al., 2020) can be expanded to *C. rubrum*.

Focusing on the CAVB population, we refined the spatial features of the red coral demographic connectivity. Over the 166 juveniles analyzed here, 27 (16.2%) were considered as migrants, suggesting that, in spite of a substantial demographic connectivity, the vast majority of the juveniles was locally produced. A high level of self-recruitment was previously suggested as a central process in red coral population dynamics (Costantini et al., 2007b; Ledoux et al., 2010b). Considering the migrant juveniles sampled in CAVB (CAVB-JUV-M), the sibship analyses revealed the occurrence sibship aggregation. We identified two pairs of halfsibs and one pair of fullsibs in these juveniles, the two individuals of the three pairs being sampled in the same quadrat. Accordingly, collective dispersal, the dispersal of at least two sibs originating from the same reproductive event in a distant population (Broquet et al., 2013), may occur in red coral. The factors driving these events are still largely unknown (but see Ottmann et al., 2016). Beside abiotic factors (e.g., no mixing of mass water), biotic factors both at the larval (behavior) and adult (synchronous larval release) levels, combined to species reproductive strategies, have been called on to explain collective dispersal. In particular, most of the collective dispersals involving marine invertebrate larvae were reported in brooding or partially brooding species (e.g., Riquet et al., 2017, but see Dubé et al., 2020). The internal fertilization (Santangelo et al., 2003), brooding period (Bramanti et al., 2005), and larvae active swimming behavior (Martínez-Quintana et al., 2015) may drive collective dispersal in red coral.

Finally, we gained a first insight into the temporal features of red coral demographic connectivity. The assignment analyses suggest a lack of constant pattern, at least for the CAVB population. In the juveniles sampled in CAVB (CAVB-JUV), most of the migrants came from DHM. This DHM to CAVB migration was not reported when considering the pool of mature colonies. Temporal variability in the genetic make-up of larvae and juveniles has been previously reported in various marine species from fishes (e.g., Salles et al., 2016) to invertebrates (e.g., David et al., 1997; Riquet et al., 2017). This result is also in line with the recruitment variability reported in red coral (Garrabou and Harmelin, 2002). Considering the overlapping generations in this species, identifying the origin of migrants in different cohorts is a challenging task that was recently successfully achieved by analyzing different recruitment events, using settlement plates (Costantini et al., 2018). In this experimental framework, genetic heterogeneity among juveniles coming from two consecutive reproductive events was revealed (Costantini et al., 2018), consistently with the temporal variations reported here.

While the link between demographic and genetic connectivity remained to be fully characterized (but see below), the characterization of red coral demographic connectivity opens new perspectives for the management of the Scandola Marine Reserve.

Spatiotemporal Genetic Structure Among Individuals in a Near-Pristine Population: Complementing the Eco-Evolutionary Feedbacks Underlying Red Coral Population Dynamics

We demonstrated a statistically significant SGS when considering the adults and the local juvenile-stage classes in CAVB, a

population with a near-pristine demographic structure (high size colonies at high density = 201 colonies*m^{-2}; Garrabou et al., 2017). A statistically significant SGS within population has been previously demonstrated in red coral (Ledoux et al., 2010b), albeit in a declining population characterized by different demographic features (high density of small size colonies; 160 colonies*m^{-2}). This shared pattern in such contrasted demographic situations suggests that SGS among colonies may be a common feature of red coral populations. Interestingly, the moment estimator of the neighborhood size (Nb) estimated in CAVB was one order of magnitude higher than the Nb previously reported in the declining population (575.3 vs. 75 individuals), resulting in a slightly lower effective dispersal (σ_g; from 15.1 to 21.4 cm vs. from 22.6 to 32.1 cm). While this comparison should be taken with caution owing to the different sampling strategies (quadrats vs. individual sampling), a decrease of σ_g with a higher effective density is expected (see Vekemans and Hardy, 2004). This feedback between effective density and dispersal (i.e., higher dispersal in low-density population) was proposed as a process buffering, to some point, the increase of genetic drift expected in declining populations and may be critical for the maintenance of red coral populations (Ledoux et al., 2020).

Such restricted σ_g seems conflicting with the pattern of demographic connectivity previously drawn based on assignment method. One should keep in mind the different dispersal components (demographic vs. genetic) estimated by the two methods (Broquet and Petit, 2009). Moreover, estimation of σ_g based on SGS among individuals may underestimate long-distance dispersal (Leblois et al., 2004). Consistent with a potential underestimation of effective dispersal, the sibship analyses revealed for instance one parent–offspring pair separated by 300 cm, suggesting that longer-distance dispersal may happen.

We then decomposed the SGS accounting for the stage class of the individuals (i.e., adults and juveniles). We first revealed a significant SGS among adults and juveniles and showed that the significant SGS was retained in the juveniles but not in the adults. The significant SGS among stage classes corroborates the central role of restricted dispersal in the structure and in the dynamics of red coral populations. In spite of the demographic connectivity among populations previously discussed and of the occurrence of long-distance dispersal events, larvae recruit preferentially in the close vicinity of their parents (Ledoux et al., 2010b, this article). This restricted dispersal builds up the SGS within local juveniles. While potential methodological limitations (i.e., overlapping generations in the adult sample; see Berens et al., 2014) may take part in the random pattern observed among adult colonies, the decrease in SGS from juveniles to adults can be linked to an imprint of mortality during the early life stage (e.g., Chung et al., 2003; Hampe et al., 2010), corroborating the high mortality rates in the juveniles compared to adults reported by demographic surveys (Garrabou and Harmelin, 2002; Bramanti et al., 2007; Santangelo et al., 2012). The process underlying this demographic transition (e.g., self-thinning vs. density-independent mortality) remains a matter of discussion in red coral (Cau et al., 2016; Garrabou et al., 2017).

Shifting From Patterns to Processes to Improve the Conservation of Red Coral in the Scandola Marine Reserve and the Restoration of Declining Populations

Implemented more than 40 years ago, the Scandola Marine Reserve belongs to the 0.23% of the Mediterranean that is fully protected (Claudet et al., 2020). Beside harboring a unique and near-pristine shallow population of red coral (Garrabou et al., 2017), the benefits of the management conducted in this MPA on red coral are noteworthy (Linares et al., 2010, 2012). We revealed here contrasted connectivity among populations forming the red coral network. We highlighted the restricted connectivity, at least on a contemporary timescale, among the Northern and Southern parts of the MPA and, accordingly, the need to consider these localities as distinct management units. The potential for genetic isolation at local scale, as observed for PLU, is also of management interest. Indeed, isolated populations may be targeted by restoration to increase their effective population size and to buffer potential drift and related negative effects (e.g., expression of deleterious alleles and decrease population fitness; see Frankham, 2005; Garner et al., 2020). Still on the management prioritization, we identified two particular populations, namely, CAVB and ALE, as the main sources of migrants within the network. Additional populations must be sampled to refine this connectivity pattern. Moreover, while our results suggested relatively homogeneous levels of genetic diversity among the different populations, this pattern does not account for adaptive genetic variations (i.e., variations that produce advantages in fitness), which may be limited in this particular area (Ledoux et al., 2015). This is a crucial knowledge gap for an effective management of the MPA, which should be filled using available genomic resources (Pratlong et al., 2015, 2018).

Restoration actions are a promising tool in red coral at local scale (Montero-Serra et al., 2017). Restoration protocols usually rely on different components including the number of individuals to transplant, the transplanting design, and the choice of source populations (Weeks et al., 2011; Mijangos et al., 2015; Breed et al., 2019). Ledoux et al. (2010b) suggest to create small size and dense patches (tens to a hundred of colonies over half square meter) of reproductive colonies to mimic the patterns of structure characterizing red coral populations. Our results support this preliminary statement. We confirmed here the importance of restricted dispersal and of interactions among genetically and spatially related individuals in the dynamics of red coral populations. The size of a functional restored patch, i.e., promoting genetic interactions among colonies, depends on the density of transplanted colonies. Interestingly, in the two contrasted density situations analyzed so far (i.e., a declining population vs. near-pristine population), the mean effective dispersal remains within the order of tens of cm, with occasional more distant dispersal events. This restricted range of dispersal distances sets the scale for restoration actions (i.e., tens of cm). Yet, the parentage analyses revealed the potential for long-distance effective dispersal within population, beyond the mean parent–offspring distance (σ_g). Accordingly, it may be more efficient to

restore a particular location creating small and dense patches of colonies (tens to a hundred of colonies in 0.5 to 1 m^2 area), separated by 2 to 3 m, in order to "capture" these long-distance dispersers, rather than a low-density and continuous patch. Finally, sourcing is a critical aspect of restoration. The identification of FGMs from different origins supports the need to consider different populations for sourcing. However, one important gap here relies on the ability of red coral colonies to deal with the ongoing warming (Garrabou et al., 2019). In this context, the identification of the genomic factors and eco-evolutionary processes driving the response to thermal stress in red coral (Pratlong et al., 2015, 2018) is the next critical step to improve restoration actions in the warming context.

Overall, the spatially integrated demo-genetic approach presented here revealed poorly known aspects of red coral eco-evolution, with strong implications for the species conservation and restoration. While targeting this species is particularly relevant considering its key ecological role in the coralligenous community, we call for the development of comparative studies among species to increase the robustness of the management inputs coming from eco-evolution studies.

DATA AVAILABILITY STATEMENT

The original contributions presented in the study are included in the article/**Supplementary Material**, further inquiries can be directed to the corresponding author/s.

AUTHOR CONTRIBUTIONS

J-BL, J-MD, and JG designed the study. J-BL, IM-S, J-MD, CL, and JG collected the samples. CG, PL-S, and J-BL performed the molecular analyses. CG and J-BL conducted the statistical analyses and led the writing of the manuscript. All authors contributed critically to the drafts and gave the final approval for publication.

FUNDING

SUPPLEMENTARY MATERIAL

The Supplementary Material for this article can be found online at: https://www.frontiersin.org/articles/10.3389/fmars. 2021.633057/full#supplementary-material

REFERENCES

Abbiati, M., Santangelo, G., and Novelli, S. (1993). Genetic variation within and between two Tyrrhenian populations of the Mediterranean alcyonarian *Corallium rubrum. Mar. Ecol. Prog. Ser.* 95, 245–250. doi: 10.3354/meps095245

Arizmendi-Mejía, R., Linares, C., Garrabou, J., Antunes, A., Ballesteros, E., Cebrian, E., et al. (2015). Combining genetic and demographic data for the conservation of a Mediterranean marine habitat-forming species. *PLoS One* 10:e0119585. doi: 10.1371/journal.pone.0119585

Aurelle, D., and Ledoux, J.-B. (2013). Interplay between isolation by distance and genetic clusters in the red coral *Corallium rubrum*: insights from simulated and empirical data. *Conserv. Genet.* 14, 705–716. doi: 10.1007/s10592-013-0464-0

Aurelle, D., Ledoux, J.-B., Rocher, C., Borsa, P., Chenuil, A., and Féral, J.-P. (2011). Phylogeography of the red coral (*Corallium rubrum*): inferences on the evolutionary history of a temperate gorgonian. *Genetica* 139, 855–869. doi: 10.1007/s10709-011-9589-6

Aurelle, D., Tariel, J., Zuberer, F., Haguenauer, A., Ribout, C., Masmoudi, M., et al. (2020). Genetic insights into recolonization processes of Mediterranean octocorals. *Mar. Biol.* 167:73. doi: 10.1007/s00227-020-03684-z

Ballesteros, E. (2006). Mediterranean coralligenous assemblages: a synthesis of present knowledge. *Oceanogr. Mar. Biol. An Annu. Rev.* 44, 123–195.

Berens, D. G., Braun, C., González-Martínez, S. C., Griebeler, E. M., Nathan, R., and Böhning-Gaese, K. (2014). Fine-scale spatial genetic dynamics over the life cycle of the tropical tree Prunus africana. *Heredity (Edinb)* 113, 401–407. doi: 10.1038/hdy.2014.40

Bierne, N., Bonhomme, F., and Arnaud-Haond, S. (2016). Editorial dedicated population genomics for the silent world: the specific questions of marine population genetics. *Curr. Zool.* 62, 545–550. doi: 10.1093/cz/zow107

Boavida, J., Paulo, D., Aurelle, D., Arnaud-Haond, S., Marschal, C., Reed, J., et al. (2016). A well-kept treasure at depth: precious red coral rediscovered in atlantic deep coral gardens (SW Portugal) after 300 Years. *PLoS One* 11:e0147228. doi: 10.1371/journal.pone.0147228

Bramanti, L., Magagnini, G., De Maio, L., and Santangelo, G. (2005). Recruitment, early survival and growth of the Mediterranean red coral *Corallium rubrum* (L 1758), a 4-year study. *J. Exp. Mar. Bio. Ecol.* 314, 69–78. doi: 10.1016/j.jembe.2004.08.029

Bramanti, L., Rossi, S., Tsounis, G., Gili, J. M., and Santangelo, G. (2007). Settlement and early survival of red coral on artificial substrates in different geographic

areas: some clues for demography and restoration. *Hydrobiologia* 580, 219–224. doi: 10.1007/s10750-006-0452-1

Breed, M. F., Harrison, P. A., Blyth, C., Byrne, M., Gaget, V., Gellie, N. J. C., et al. (2019). The potential of genomics for restoring ecosystems and biodiversity. *Nat. Rev. Genet.* 20, 615–628. doi: 10.1038/s41576-019-0152-0

Broquet, T., and Petit, E. J. (2009). Molecular estimation of dispersal for ecology and population genetics. *Annu. Rev. Ecol. Evol. Syst.* 40, 193–216. doi: 10.1146/annurev.ecolsys.110308.120324

Broquet, T., Viard, F., and Yearsley, J. M. (2013). Genetic drift and collective dispersal can result in chaotic genetic patchiness. *Evolution (N. Y)* 67, 1660–1675. doi: 10.1111/j.1558-5646.2012.01826.x

Bruckner, A. W. (2009). Rate and extent of decline in Corallium (pink and red coral) populations: existing data meet the requirements for a CITES Appendix II listing. *Mar. Ecol. Prog. Ser.* 397, 319–332. doi: 10.3354/meps08110

Cau, A., Bramanti, L., Cannas, R., Follesa, M. C., Angiolillo, M., Canese, S., et al. (2016). Habitat constraints and self-thinning shape Mediterranean red coral deep population structure: implications for conservation practice. *Sci. Rep.* 6:23322. doi: 10.1038/srep23322

Cerrano, C., Bavestrello, G., Bianchi, C. N., Cattaneo-vietti, R., Bava, S., Morganti, C., et al. (2000). A catastrophic mass-mortality episode of gorgonians and other organisms in the Ligurian Sea (North-western Mediterranean), summer 1999. *Ecol. Lett.* 3, 284–293. doi: 10.1046/j.1461-0248.2000.00152.x

Chung, M. Y., Epperson, B. K., and Chung, M. (2003). Genetic structure of age classes in *Camellia japonica* (Theaceae). *Evolution* 57, 62–73. doi: 10.1111/j.0014-3820.2003.tb00216.x

Chung, M., Nason, J., Nason, J., Nason, J., Nason, J., and Nason, J. (2007). Spatial demographic and genetic consequences of harvesting within populations of the terrestrial orchid *Cymbidium goeringii*. *Biol. Conserv.* 137, 125–137.

Claudet, J., Loiseau, C., Sostres, M., and Correspondence, M. Z. (2020). Underprotected marine protected areas in a global biodiversity hotspot. *One Earth* 2, 380–384. doi: 10.1016/j.oneear.2020.03.008

Cook, C. N., and Sgrò, C. M. (2018). Understanding managers' and scientists' perspectives on opportunities to achieve more evolutionarily enlightened management in conservation. *Evol. Appl.* 11, 1371–1388. doi: 10.1111/eva.12631

Costantini, F., Fauvelot, C., and Abbiati, M. (2007a). Genetic structuring of the temperate gorgonian coral (*Corallium rubrum*) across the western Mediterranean Sea revealed by microsatellites and nuclear sequences. *Mol. Ecol.* 16, 5168–5182.

Costantini, F., Fauvelot, C., and Abbiati, M. (2007b). Fine-scale genetic structuring in *Corallium rubrum*: evidence of inbreeding and limited effective larval dispersal. *Mar. Ecol. Prog. Ser.* 340, 109–119.

Costantini, F., Rugiu, L., Cerrano, C., and Abbiati, M. (2018). Living upside down: patterns of red coral settlement in a cave. *PeerJ* 6:e4649. doi: 10.7717/peerj.4649

Costello, M. J., and Ballantine, B. (2015). Biodiversity conservation should focus on no-take marine reserves: 94% of marine protected areas allow fishing. *Trends Ecol. Evol.* 30, 507–509. doi: 10.1016/j.tree.2015.06.011

Cramer, W., Guiot, J., Fader, M., Garrabou, J., Gattuso, J.-P., Iglesias, A., et al. (2018). Climate change and interconnected risks to sustainable development in the Mediterranean. *Nat. Clim. Chang.* 8, 972–980. doi: 10.1038/s41558-018-0299-2

Crisci, C., Ledoux, J.-B., Mokhtar-Jamaï, K., Bally, M., Bensoussan, N., Aurelle, D., et al. (2017). Regional and local environmental conditions do not shape the response to warming of a marine habitat-forming species /631/158 /631/208/457 /45/23 /45 /141 article. *Sci. Rep.* 7:5069. doi: 10.1038/s41598-017-05220-4

David, P., Perdieu, M.-A., Pernot, A.-F., and Jarne, P. (1997). Fine-Grained spatial and temporal population genetic structure in the marine bivalve *Spisula ovalis*. *Evolution* 51:1318. doi: 10.2307/2411061

Diffenbaugh, N. S., Pal, J. S., Giorgi, F., and Gao, X. (2007). Heat stress intensification in the Mediterranean climate change hotspot. *Geophys. Res. Lett.* 34, L11706. doi: 10.1029/2007GL030000

Dubé, C. E., Boissin, E., Mercière, A., and Planes, S. (2020). Parentage analyses identify local dispersal events and sibling aggregations in a natural population of *Millepora* hydrocorals, a free-spawning marine invertebrate. *Mol. Ecol.* 29, 1508–1522. doi: 10.1111/mec.15418

Edgar, G. J., Stuart-Smith, R. D., Willis, T. J., Kininmonth, S., Baker, S. C., Banks, S., et al. (2014). Global conservation outcomes depend on marine protected areas with five key features. *Nature* 506, 216–220. doi: 10.1038/nature13022

Evanno, G., Regnaut, S., and Goudet, J. (2005). Detecting the number of clusters of individuals using the software STRUCTURE: a simulation study. *Mol. Ecol.* 14, 2611–2620. doi: 10.1111/j.1365-294X.2005.02553.x

Falush, D., Stephens, M., and Pritchard, J. (2003). Inference of population structure using multilocus genotype data: linked loci and correlated allele frequencies. *Genetics* 164, 1567–1587.

Falush, D., Stephens, M., and Pritchard, J. K. (2007). Inference of population structure using multilocus genotype data: dominant markers and null alleles. *Mol. Ecol. Notes* 7, 574–578. doi: 10.1111/j.1471-8286.2007.01758.x

Foll, M., and Gaggiotti, O. (2006). Identifying the environmental factors that determine the genetic structure of populations. *Genetics* 174, 875–891. doi: 10.1534/genetics.106.059451

Frankham, R. (2005). Genetics and extinction. *Biol. Conserv.* 126, 131–140. doi: 10.1016/j.biocon.2005.05.002

Gaggiotti, O. E., and Foll, M. (2010). Quantifying population structure using the F-model. *Mol. Ecol. Resour.* 10, 821–830. doi: 10.1111/j.1755-0998.2010.02873.x

Gagnaire, P., Broquet, T., Aurelle, D., Viard, F., Souissi, A., Bonhomme, F., et al. (2015). Using neutral, selected, and hitchhiker loci to assess connectivity of marine populations in the genomic era. *Evol. Appl.* 8, 769–786. doi: 10.1111/eva.12288

Garner, B. A., Hoban, S., and Luikart, G. (2020). IUCN Red List and the value of integrating genetics. *Conserv. Genet.* 21, 795–801. doi: 10.1007/s10592-020-01301-6

Garrabou, J., and Harmelin, J. G. (2002). A 20-year study on life-history traits of a harvested long-lived temperate coral in the NW Mediterranean: insights into conservation and management needs. *J. Anim. Ecol.* 71, 966–978. doi: 10.1046/j.1365-2656.2002.00661.x

Garrabou, J., Coma, R., Bensoussan, N., Bally, M., Chevaldonné, P., Cigliano, M., et al. (2009). Mass mortality in Northwestern Mediterranean rocky benthic communities: effects of the 2003 heat wave. *Glob. Chang. Biol.* 15, 1090–1103. doi: 10.1111/j.1365-2486.2008.01823.x

Garrabou, J., Gómez-Gras, D., Ledoux, J.-B., Linares, C., Bensoussan, N., López-Sendino, P., et al. (2019). Collaborative database to track mass mortality events in the Mediterranean Sea. *Front. Mar. Sci.* 6:707. doi: 10.3389/fmars.2019.00707

Garrabou, J., Perez, T., Sartoretto, S., and Harmelin, J. G. (2001). Mass mortality event in red coral *Corallium rubrum* populations in the Provence region (France, NW Mediterranean). *Mar. Ecol. Prog. Ser.* 217, 263–272. doi: 10.3354/meps217263

Garrabou, J., Sala, E., Linares, C., Ledoux, J. B., Montero-Serra, I., Dominici, J. M., et al. (2017). Re-shifting the ecological baseline for the overexploited Mediterranean red coral. *Sci. Rep.* 7:42404. doi: 10.1038/srep42404

Gómez-Gras, D., Linares, C., Dornelas, M., Madin, J. S., Brambilla, V., Ledoux, J.-B., et al. (2021). Climate change transforms the functional identity of Mediterranean coralligenous assemblages. *Ecol. Lett.* 24, 1038–1051. doi: 10.1111/ele.13718

Gorospe, K. D., and Karl, S. A. (2013). Genetic relatedness does not retain spatial pattern across multiple spatial scales: dispersal and colonization in the coral, Pocillopora damicornis. *Mol. Ecol.* 22, 3721–3736. doi: 10.1111/mec.12335

Guo, S. W., and Thompson, E. A. (1992). Performing the exact test of hardy-weinberg proportion for multiple alleles. *Biometrics* 48:361. doi: 10.2307/2532296

Hailer, F., Helander, B., Folkestad, A. O., Ganusevich, S. A., Garstad, S., Hauff, P., et al. (2006). Bottlenecked but long-lived: high genetic diversity retained in white-tailed eagles upon recovery from population decline. *Biol. Lett.* 2, 316–319. doi: 10.1098/rsbl.2006.0453

Hampe, A., El Masri, L., and Petit, R. J. (2010). Origin of spatial genetic structure in an expanding oak population. *Mol. Ecol.* 19, 459–471. doi: 10.1111/j.1365-294X.2009.04492.x

Hardy, O. J., and Vekemans, X. (2002). spagedi: a versatile computer program to analyse spatial genetic structure at the individual or population levels. *Mol. Ecol. Notes* 2, 618–620. doi: 10.1046/j.1471-8286.2002.00305.x

Jacquemyn, H., Brys, R., Vandepitte, K., Honnay, O., and Roldán-Ruiz, I. (2006). Fine-scale genetic structure of life history stages in the food-deceptive orchid *Orchis purpurea*. *Mol. Ecol.* 15, 2801–2808. doi: 10.1111/j.1365-294X.2006.02978.x

Jakobsson, M., and Rosenberg, N. A. (2007). CLUMPP: a cluster matching and permutation program for dealing with label switching and multimodality in analysis of population structure. *Bioinformatics* 23, 1801–1806. doi: 10.1093/bioinformatics/btm233

Jombart, T. (2008). adegenet: a R package for the multivariate analysis of genetic markers. *Bioinformatics* 24, 1403–1405. doi: 10.1093/bioinformatics/btn129

Jombart, T., Devillard, S., and Balloux, F. (2010). Discriminant analysis of principal components: a new method for the analysis of genetically structured populations. *BMC Genet.* 11:94. doi: 10.1186/1471-2156-11-94

Jones, O. R., and Wang, J. (2010). COLONY: a program for parentage and sibship inference from multilocus genotype data. *Mol. Ecol. Resour.* 10, 551–555. doi: 10.1111/j.1755-0998.2009.02787.x

Kalinowski, S. T., Wagner, A. P., and Taper, M. L. (2006). ml-relate: a computer program for maximum likelihood estimation of relatedness and relationship. *Mol. Ecol. Notes* 6, 576–579. doi: 10.1111/j.1471-8286.2006.01256.x

Kalisz, S., Nason, J. D., Hanzawa, F. M., and Tonsor, S. J. (2001). Spatial population genetic structure in *Trillium grandiflorum*: the roles of dispersal, mating, history and selection. *Evolution* 55, 1560–1568. doi: 10.1111/j.0014-3820.2001.tb00675.x

Knittweis, L., Aguilar, R., Alvarez, H., Borg, J. A., Evans, J., Garcia, S., et al. (2016). "New depth record of the precious red coral *Corallium rubrum*," in *Proceedings of the CIESM (Commission Internationale pour l'Exploration Scientifique de la Mer Méditerranée)*, Vol. 41, Monaco, 467.

Laikre, L., Hoban, S., Bruford, M. W., Segelbacher, G., Allendorf, F. W., Gajardo, G., et al. (2020). Post-2020 goals overlook genetic diversity. *Science* 367, 1083–1085. doi: 10.1126/science.abb2748

Leblois, R., Rousset, F., and Estoup, A. (2004). Influence of spatial and temporal heterogeneities on the estimation of demographic parameters in a continuous population using individual microsatellite data. *Genetics* 166, 1081–1092. doi: 10.1534/genetics.166.2.1081

Ledoux, J., Aurelle, D., Bensoussan, N., Marschal, C., Feral, J., and Garrabou, J. (2015). Potential for adaptive evolution at species range margins: contrasting interactions between red coral populations and their environment in a changing ocean. *Ecol. Evol* 5, 1178–1192. doi: 10.1002/ece3.1324

Ledoux, J., Frias-Vidal, S., Montero-Serra, I., Antunes, A., Casado Bueno, C., Civit, S., et al. (2020). Assessing the impact of population decline on mating system in the overexploited Mediterranean red coral. *Aquat. Conserv. Mar. Freshw. Ecosyst.* 30, 1149–1159. doi: 10.1002/aqc.3327

Ledoux, J.-B., Frleta-Valić, M., Kipson, S., Antunes, A., Cebrian, E., Linares, C., et al. (2018). Postglacial range expansion shaped the spatial genetic structure in a marine habitat-forming species: implications for conservation plans in the Eastern Adriatic Sea. *J. Biogeogr.* 45, 2645–2657. doi: 10.1111/jbi.13461

Ledoux, J.-B., Garrabou, J., Bianchimani, O., Drap, P., Féral, J.-P., and Aurelle, D. (2010a). Fine-scale genetic structure and inferences on population biology in the threatened Mediterranean red coral, *Corallium rubrum*. *Mol. Ecol.* 19, 4204–4216. doi: 10.1111/j.1365-294X.2010.04814.x

Ledoux, J.-B., Mokhtar-Jamaï, K., Roby, C., Féral, J.-P., Garrabou, J., and Aurelle, D. (2010b). Genetic survey of shallow populations of the Mediterranean red coral [*Corallium rubrum* (Linnaeus, 1758)]: new insights into evolutionary processes shaping nuclear diversity and implications for conservation. *Mol. Ecol.* 19, 675–690. doi: 10.1111/j.1365-294X.2009.04516.x

Linares, C., Bianchimani, O., Torrents, O., Marschal, C., Drap, P., and Garrabou, J. (2010). Marine protected areas and the conservation of long-lived marine invertebrates: the Mediterranean red coral. *Mar. Ecol. Prog. Ser.* 402, 69–79. doi: 10.3354/meps08436

Linares, C., Garrabou, J., Hereu, B., Diaz, D., Marschal, C., Sala, E., et al. (2012). Assessing the effectiveness of marine reserves on unsustainably harvested long-lived sessile invertebrates. *Conserv. Biol.* 26, 88–96. doi: 10.1111/j.1523-1739.2011.01795.x

Loiselle, B. A., Sork, V. L., Nason, J., and Graham, C. (1995). Spatial genetic structure of a tropical understory shrub, *Psychotria officinalis* (Rubiaceae). *Am. J. Bot.* 82:1420. doi: 10.2307/2445869

Lowe, W. H., and Allendorf, F. W. (2010). What can genetics tell us about population connectivity? *Mol. Ecol.* 19, 3038–3051. doi: 10.1111/j.1365-294X.2010.04688.x

Lukoschek, V., Riginos, C., and van Oppen, M. J. H. (2016). Congruent patterns of connectivity can inform management for broadcast spawning corals on the Great Barrier Reef. *Mol. Ecol.* 25, 3065–3080. doi: 10.1111/mec.13649

Marschal, C., Garrabou, J., Harmelin, J. G., and Pichon, M. (2004). A new method for measuring growth and age in the precious red coral Corallium rubrum (L.). *Coral Reefs* 23, 423–432. doi: 10.1007/s00338-004-0398-6

Martínez-Quintana, A., Bramanti, L., Viladrich, N., Rossi, S., and Guizien, K. (2015). Quantification of larval traits driving connectivity: the case of *Corallium rubrum* (L. 1758). *Mar. Biol.* 162, 309–318. doi: 10.1007/s00227-014-2599-z

Mijangos, J. L., Pacioni, C., Spencer, P. B. S., and Craig, M. D. (2015). Contribution of genetics to ecological restoration. *Mol. Ecol.* 24, 22–37. doi: 10.1111/mec.12995

Mokhtar-Jamaï, K., Pascual, M., Ledoux, J.-B., Coma, R., Féral, J.-P., Garrabou, J., et al. (2011). From global to local genetic structuring in the red gorgonian *Paramuricea clavata*: the interplay between oceanographic conditions and limited larval dispersal. *Mol. Ecol.* 20, 3291–3305. doi: 10.1111/j.1365-294X.2011.05176.x

Montero-Serra, I., Garrabou, J., Doak, D. F., Figuerola, L., Hereu, B., Ledoux, J.-B., et al. (2017). Accounting for life-history strategies and timescales in marine restoration. *Conserv. Lett.* 11:e12341. doi: 10.1111/conl.12341

Montero-Serra, I., Garrabou, J., Doak, D. F., Ledoux, J., and Linares, C. (2019). Marine protected areas enhance structural complexity but do not buffer the consequences of ocean warming for an overexploited precious coral. *J. Appl. Ecol.* 56, 1063–1074. doi: 10.1111/1365-2664.13321

Montero-Serra, I., Linares, C., Doak, D. F., Ledoux, J. B., and Garrabou, J. (2018). Strong linkages between depth, longevity and demographic stability across marine sessile species. *Proc. R. Soc. Lond. B Biol. Sci.* 285:20172688. doi: 10.1098/rspb.2017.2688

Montero-Serra, I., Linares, C., García, M., Pancaldi, F., Frleta-Valić, M., Ledoux, J.-B., et al. (2015). Harvesting effects, recovery mechanisms, and management strategies for a long-lived and structural precious coral. *PLoS One* 10:e0117250. doi: 10.1371/journal.pone.0117250

Nei, M. (1973). Analysis of gene diversity in subdivided populations. *Proc. Natl. Acad. Sci. U.S.A.* 70, 3321–3323. doi: 10.1073/pnas.70.12.3321

Ottmann, D., Grorud-Colvert, K., Sard, N. M., Huntington, B. E., Banks, M. A., and Sponaugle, S. (2016). Long-term aggregation of larval fish siblings during dispersal along an open coast. *Proc. Natl. Acad. Sci. U.S.A.* 113, 14067–14072. doi: 10.1073/pnas.1613440113

Padrón, M., Costantini, F., Bramanti, L., Guizien, K., and Abbiati, M. (2018). Genetic connectivity supports recovery of gorgonian populations affected by climate change. *Aquat. Conserv. Mar. Freshw. Ecosyst.* 28, 776–787. doi: 10.1002/aqc.2912

Palumbi, S. R. (2004). Marine reserves and ocean neighborhodds: the spatial scale of marine populations and their management. *Annu. Rev. Environ. Resour.* 29, 31–68. doi: 10.1146/annurev.energy.29.062403.102254

Pardini, E. A., and Hamrick, J. L. (2008). Inferring recruitment history from spatial genetic structure within populations of the colonizing tree *Albizia julibrissin* (Fabaceae). *Mol. Ecol.* 17, 2865–2879. doi: 10.1111/j.1365-294X.2008.03807.x

Petit, R. J., El Mousadik, A., and Pons, O. (1998). Identifying populations for conservation on the basis of genetic markers. *Conserv. Biol.* 12, 844–855. doi: 10.1046/j.1523-1739.1998.96489.x

Pew, J., Muir, P. H., Wang, J., and Frasier, T. R. (2015). Related: an R package for analysing pairwise relatedness from codominant molecular markers. *Mol. Ecol. Resour.* 15, 557–561. doi: 10.1111/1755-0998.12323

Piry, S., Alapetite, A., Cornuet, J.-M., Paetkau, D., Baudouin, L., and Estoup, A. (2004). GENECLASS2: a software for genetic assignment and first-generation migrant detection. *J. Hered.* 95, 536–539. doi: 10.1093/jhered/esh074

Pratlong, M., Haguenauer, A., Brener, K., Mitta, G., Toulza, E., Garrabou, J., et al. (2018). Separate the wheat from the chaff: genomic scan for local adaptation in the red coral *Corallium rubrum*. *Peer Community Evol. Biol* Available online at: https://hal.archives-ouvertes.fr/hal-01974422 (accessed November 15, 2020).

Pratlong, M., Haguenauer, A., Chabrol, O., Klopp, C., Pontarotti, P., and Aurelle, D. (2015). The red coral (*Corallium rubrum*) transcriptome: a new resource for population genetics and local adaptation studies. *Mol. Ecol. Resour.* 15, 1205–1215. doi: 10.1111/1755-0998.12383

Pritchard, J., Stephens, M., and Donnelly, P. (2000). Inference of population structure using multilocus genotype data. *Genetics* 155, 945–959.

Puechmaille, S. J. (2016). The program structure does not reliably recover the correct population structure when sampling is uneven: subsampling and new estimators alleviate the problem. *Mol. Ecol. Resour.* 16, 608–627. doi: 10.1111/1755-0998.12512

Rannala, B., and Mountain, J. L. (1997). Detecting immigration by using multilocus genotypes. *Proc. Natl. Acad. Sci. U.S.A.* 94, 9197–9201.

Riquet, F., Comtet, T., Broquet, T., and Viard, F. (2017). Unexpected collective larval dispersal but little support for sweepstakes reproductive success in the highly dispersive brooding mollusc *Crepidula fornicata*. *Mol. Ecol.* 26, 5467–5483. doi: 10.1111/mec.14328

Rosenberg, N. A. (2003). Distruct: a program for the graphical display of population structure. *Mol. Ecol. Notes* 4, 137–138. doi: 10.1046/j.1471-8286.2003.00566.x

Rousset, F. (1997). Genetic differentiation and estimation of gene flow from F-statistics under isolation by distance. *Genetics* 145, 1219–1228.

Rousset, F. (2008). genepop'007: a complete re-implementation of the genepop software for Windows and Linux. *Mol. Ecol. Resour.* 8, 103–106. doi: 10.1111/j.1471-8286.2007.01931.x

Rousset (2000). Genetic differentiation between individuals. *J. Evol. Biol.* 13, 58–62. doi: 10.1046/j.1420-9101.2000.00137.x

Santangelo, G., Abbiati, M., Giannini, F., and Cicogna, F. (1993). Red coral fishing trends in the western Mediterranean Sea. *Sci. Mar.* 57, 139–143.

Sale, P. F., Cowen, R. K., Danilowicz, B. S., Jones, G. P., Kritzer, J. P., Lindeman, K. C., et al. (2005). Critical science gaps impede use of no-take fishery reserves. *Trends Ecol. Evol.* 20, 74–80. doi: 10.1016/j.tree.2004.11.007

Salles, O. C., Pujol, B., Maynard, J. A., Almany, G. R., Berumen, M. L., Jones, G. P., et al. (2016). First genealogy for a wild marine fish population reveals multigenerational philopatry. *Proc. Natl. Acad. Sci. U.S.A.* 113, 13245–13250. doi: 10.1073/pnas.1611797113

Santangelo, G., Bramanti, L., Rossi, S., Tsounis, G., Vielmini, I., Lott, C., et al. (2012). Patterns of variation in recruitment and post-recruitment processes of the Mediterranean precious gorgonian coral *Corallium rubrum*. *J. Exp. Mar. Biol. Ecol* 411, 7–13. doi: 10.1016/J.JEMBE.2011.10.030

Santangelo, G., Carletti, E., Maggi, E., and Bramanti, L. (2003). Reproduction and population sexual structure of the overexploited Mediterranean red coral *Corallium rubrum*. *Mar. Ecol. Prog. Ser.* 248, 99–108. doi: 10.3354/meps248099

Soulé, M. (1985). What is conservation biology? *Bioscience* 35, 727–734.

Torrents, O., Garrabou, J., Marschal, C., and Harmelin, J. G. (2005). Age and size at first reproduction in the commercially exploited red coral *Corallium rubrum* (L.) in the Marseilles area (France, NW Mediterranean). *Biol. Conserv.* 121, 391–397. doi: 10.1016/j.biocon.2004.05.010

Vekemans, X., and Hardy, O. J. (2004). New insights from fine-scale spatial genetic structure analyses in plant populations. *Mol. Ecol.* 13, 921–935. doi: 10.1046/j.1365-294x.2004.02076.x

Wang, J. (2017). The computer program structure for assigning individuals to populations: easy to use but easier to misuse. *Mol. Ecol. Resour.* 17, 981–990. doi: 10.1111/1755-0998.12650

Waples, R. S., and Gaggiotti, O. (2006). What is a population? An empirical evaluation of some genetic methods for identifying the number of gene pools and their degree of connectivity. *Mol. Ecol.* 15, 1419–1439. doi: 10.1111/j.1365-294X.2006.02890.x

Weeks, A. R., Sgro, C. M., Young, A. G., Frankham, R., Mitchell, N. J., Miller, K. A., et al. (2011). Assessing the benefits and risks of translocations in changing environments: a genetic perspective. *Evol. Appl.* 4, 709–725. doi: 10.1111/j.1752-4571.2011.00192.x

Weir, B. S., and Cockerham, C. C. (1984). Estimating F-statistics for the analysis of population structure. *Evolution (N. Y)* 38:1358. doi: 10.2307/2408641

Zibrowius, H., Monteiro-Marques, V., and Grasshoff, M. (1984). La répartition du *Corallium rubrum* dans l'Atlantique (Cnidaria: Anthozoa: Gorgonaria). *Téthys* 11, 163–170.